Pseudo-Dynamic Testing of Unreinforced Masonry Building with Flexible Diaphragm

Jocelyn Paquette[1] and Michel Bruneau, M. ASCE[2]

Abstract: To complement the computer simulations, component testing, and small-scale shake table tests done by other researchers, a full-scale one-story unreinforced brick masonry specimen having a wood diaphragm was subjected to earthquake excitations using pseudo-dynamic testing. The specimen was designed to better understand the flexible-floor/rigid-wall interaction, the impact of wall continuity at the building corners and the effect of a relatively weak diaphragm on the expected seismic behavior. This paper reports on the characteristics of the specimen and the analyses of the dynamic response of the shear walls with piers having a rocking and/or a sliding behavior. These results are compared with predictions from existing seismic evaluation methodologies. It is found that the overall building was relatively resilient to earthquake excitation, even though cracking was extensive, and that some (but not all) of the existing seismic evaluation methodologies accurately capture the rocking/sliding behavior that developed in the shear walls under large displacement.

DOI: 10.1061/(ASCE)0733-9445(2003)129:6(708)

CE Database subject headings: Masonry; Seismic response; Earthquakes; Tests.

Introduction

The Uniform Code for Building Conservation (UCBC) (ICBO 1997) *Seismic Strengthening Provisions for Unreinforced Masonry Bearing Wall Buildings* presents a systematic procedure for the evaluation and seismic strengthening of buildings having unreinforced masonry (URM) bearing walls and flexible floor/roof diaphragms. This special procedure, adapted from one developed by the ABK joint venture (ABK 1984; FEMA 1992; Bruneau 1994a,b) and used extensively in the Los Angeles area, has made it economically possible to significantly reduce the seismic hazard posed by these buildings, as evidenced by the considerably less damage suffered by seismically retrofitted URM buildings in recent earthquakes, compared to nonretrofitted ones (Bruneau 1990, 1995; Rutherford and Chekene 1991). However, even though this procedure is founded on extensive component testing, full-scale testing of an entire URM building having wood diaphragms has not been conducted. Such a test would also complement the computer simulations and small-scale shake table tests by other researchers (Costley and Abrams 1995).

The writers conducted one such test on a full-scale 4.1 m $\times$ 5.7 m $\times$ 2.7 m single-story URM building designed to better understand the flexible-floor/rigid-wall interaction and the impact of wall continuity at the building corners on the expected seismic behavior. This paper presents the characteristics of the specimen, the concepts underlying its design, and the results from these tests for the shear walls as compared with expected performance predicted by different codified equations, notably those from the FEMA 273 and 306 documents.

[1]Conservation Engineer, Heritage Conservation Program, Public Works and Government Services Canada, 25 Eddy, Hull, Québec, Canada K1A 0M5. E-mail: Jocelyn.Paquette@pwgsc.gc.ca

[2]Professor and Deputy Director, Multi-Disciplinary Centre for Earthquake Engineering Research, Dept. of Civil and Environmental Engineering, 130 Ketter Hall, State Univ. of New York, Buffalo, NY 14260. E-mail: bruneau@acsu.buffalo.edu

Note. Associate Editor: Brad Cross. Discussion open until November 1, 2003. Separate discussions must be submitted for individual papers. To extend the closing date by one month, a written request must be filed with the ASCE Managing Editor. The manuscript for this paper was submitted for review and possible publication on August 3, 2001; approved on July 31, 2002. This paper is part of the ***Journal of Structural Engineering***, Vol. 129, No. 6, June 1, 2003. ©ASCE, ISSN 0733-9445/2003/6-708–716/$18.00.

Design and Description of Specimen

Objectives and Constraints

The design of the unreinforced masonry specimen was dictated by several objectives and constraints. First, the piers were designed to all undergo rocking, but with aspect ratios (and rocking resistance) that varied as much as possible. Second, an important objective was to choose an adequate wood floor diaphragm that would yield while piers are rocking, in order to investigate the postulate that a weak floor diaphragm is desirable to limit the force transmitted to the shear walls.

Assuming the newly constructed specimen to be in pristine condition prior to testing (which may not be necessarily the case in an old existing building), calculations showed that piers would first crack, followed by a drop in lateral load resistance stabilizing at the rocking strength, before the rocking mechanism could develop. Hence, it was decided to make the tested shear walls load bearing to reduce their cracking-strength-to-rocking-strength ratios. A sufficiently strong diaphragm also had to be provided to attain the cracking loads which limited the amount of diaphragm inelastic behavior that could develop once rocking occurs.

Finally, the overall dimensions of the specimen were also limited by the space available in the structure laboratory, and the maximum size (38 mm $\times$ 286 mm) and length (6.1 m) of wood joists readily available for construction of the wood diaphragm.

Description of Specimen

As shown in Figs. 1, 2, and 3, the full-scale single-story unreinforced building specimen was approximately 4 m $\times$ 5.6 m in plan, with wall height and thickness of 2.7 m and 190 mm, respec-

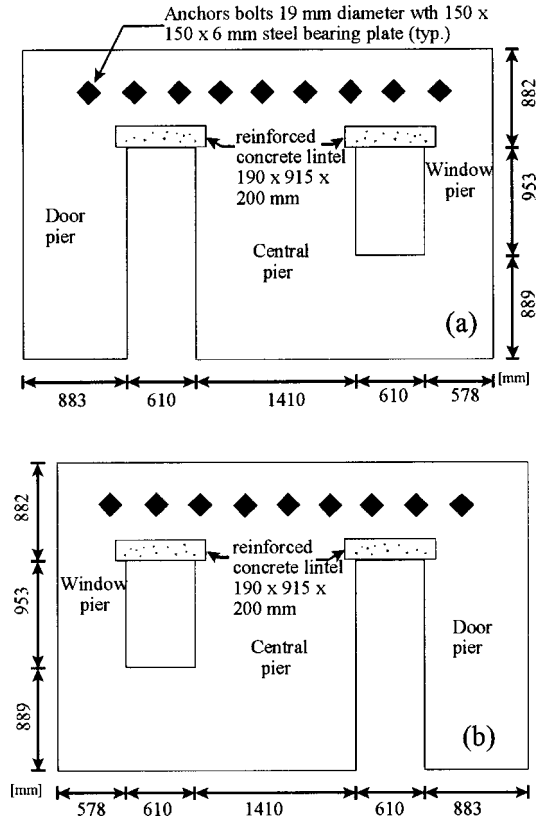

Fig. 1. Elevation of URM specimen (parallel to loading): (a) east wall and (b) west wall

tively. Dimensions of the load-bearing shear walls (4 m×2.7 m) limited the practical number of openings to two: a window and a door, as shown in Fig. 4. Shear walls were designed such that all piers would successively develop a pier-rocking behavior during seismic response, as shown in Fig. 5. This rigid-body mechanism is recognized by the UCBC to be a favorable stable failure mechanism.

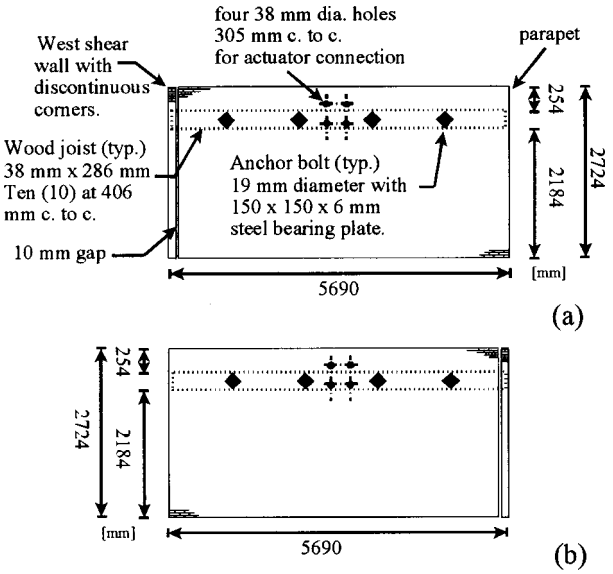

Fig. 2. Elevation of URM specimen (normal to loading): (a) south wall and (b) north wall

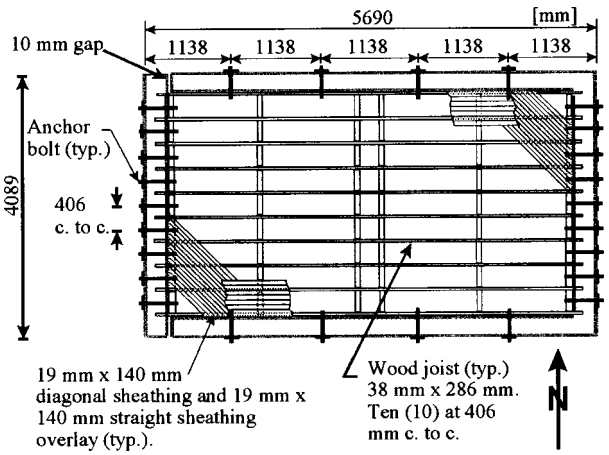

Fig. 3. Wood sheathed diaphragm framing details

A diagonal board plus straight sheathing overlay diaphragm was selected. It was designed to be sufficiently strong to resist the larger lateral load required to crack the masonry walls, and still provide some inelastic deformation during the pier-rocking behavior.

Among noteworthy features of this specimen, two corners (west shear wall) of the building were built discontinuous, with vertical gaps left between the shear wall and its perpendicular walls. This permits a comparison between the plane models considered by many engineers and the actual behavior of building corners, and allows us to assess the significance of this discrepancy on seismic performance, particularly when piers are subjected to rocking.

Construction and Material Properties

A rectangular reinforced concrete pad was designed and constructed to provide a foundation for the specimen. No mechanical connectors were used between the foundation and specimen. Using skilled bricklayers, the two wythes solid brick walls (collar joint filled) were laid in running and American bond, with a header course at every sixth course, tying the two wythes together. The bricks used were standard metric modular 90 mm ×57 mm×190 mm. Type O mortar was used to replicate old construction methods and materials with cement:lime:sand in 1:2:9 proportion.

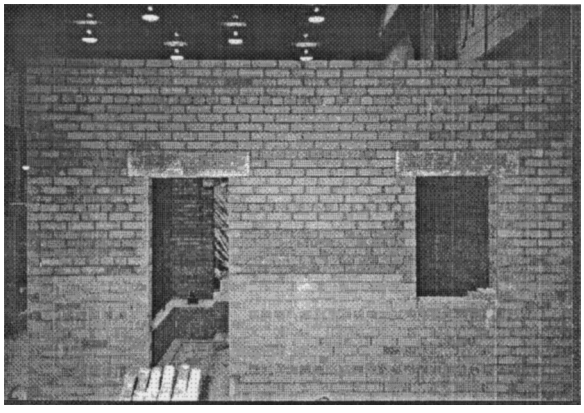

Fig. 4. URM specimen

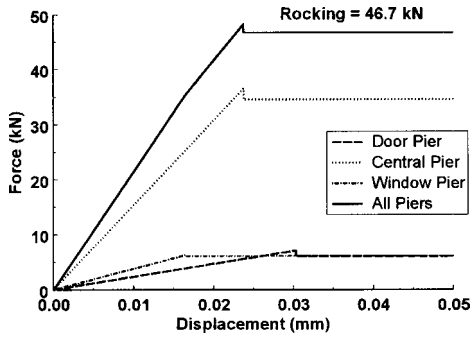

Fig. 5. Pier rocking resistance

Wood Diaphragm

The specimen has a flexible diaphragm constructed with wood joists covered with diagonal boards with a straight board overlay. All framing and sheathing lumber were construction grade spruce, and common 8*d* nails were used. The ten 38 mm×286 mm joists at 406 mm on center were supported by the interior wythe of the masonry, and 38 mm×286 mm blockings were provided between joists at each end, and 38 mm×89 mm at 1.22 m on center elsewhere. The diagonal and straight sheathings consisted of 19 mm ×140 mm boards, joined with three nails at ends of each board and two nails at all other support. The diaphragm was anchored to the walls with through-wall bolts in accordance to the special procedure of the UCBC. A parapet was built above the wood joist, and an additional gravity load on the diaphragm was provided by plastic containers filled with water, simulating a 2.4 kPa live load.

Masonry Properties

Masonry properties were obtained from simple component tests. The brick and mortar compressive strengths were determined by crushing five half-bricks and five mortar cubes, respectively. The resulting compressive strengths of the brick (f'_{br}) and mortar (f'_{mort}) were 109 and 9.24 MPa, respectively. Brick prisms were made during construction of the specimen. Five prisms consisting of five-stacked-bricks with mortar joints in between were tested in compression, while five seven-stacked-brick prisms were used in a three-point flexural bending test to determine the tensile strength of the masonry. The resulting compressive (f'_m) and tensile (f_t) strengths of the masonry were 22.2 and 0.18 MPa, respectively. A modulus of elasticity of masonry, E_m, of 850 f'_m MPa=18,870 MPa was assumed [which is less than the maximum of 20,000 MPa permitted by CSA (1994)]. To provide an estimate of the mortar shear strength along bed joints, five triplet components were tested, and four in-place shear tests were performed directly on the specimen after testing. The obtained shear strength for triplet tests and in-place shear tests were 0.52 and 0.418 MPa, respectively.

Theoretical Response

Evaluation Procedure

The seismic evaluation and strengthening of unreinforced masonry bearing wall buildings is addressed specifically in various documents such as the ''Uniform code for building conservation'' (UCBC) (ICBO 1997), the ''NEHRP handbook for seismic evaluation of existing buildings'' (FEMA 178) (FEMA 178 1992), the ''Canadian guidelines for seismic evaluation of existing buildings'' (CGSEEB) (NRC 1992), the ''NEHRP guidelines for the seismic rehabilitation of buildings'' (FEMA 273) (FEMA 273 1997), and FEMA 306 (FEMA 306 1999a) titled, ''Evaluation of earthquake damaged concrete and masonry wall buildings.''

The evaluation of URM walls subjected to lateral forces applied in-plane is performed by calculating the capacities corresponding to each possible individual modes of behavior, the lowest value being the governing failure mode. All behavior modes described below, are summarized in Table 1, showing in which documents they are addressed.

Pier Rocking

As the lateral force is increased, flexural cracks will develop along a bed joint at the top and base of a relatively slender wall, and the pier will start to rock. The rocking capacity is given by

$$V_r = 0.9\alpha P_{CE}\frac{L}{h_{\text{eff}}} \tag{1}$$

where α = factor equal to 0.5 for fixed-free cantilever wall, or equal to 1.0 for a fixed-fixed pier; P_{CE} = expected vertical axial compressive force; L = pier's width; and h_{eff} = effective height reflecting crack patterns.

Eq. (1) is found in FEMA 273, FEMA 306, and in a similar form in FEMA 178, the CGSEEB, and UCBC 1997, where D and H are used for the pier's width and height, respectively.

Sliding Shear Resistance

For squat walls, a diagonal shear crack can develop through bed and head mortar joints. Neglecting the tensile capacity of the head joint, the horizontal stair-stepped shear capacity of a pier having such cracking is given by

$$V_a = v_m\frac{Dt}{1.5} \tag{2}$$

Table 1. Possible Lateral Behavior Modes as Per Different Codes and Methodologies

Modes of behavior	Federal Emergency Management Agency 178	Canadian Guidelines for the Seismic Evaluation of Existing Buildings	Uniform Code for Building Conservation 1997	Federal Emergency Management Agency 273	Federal Emergency Management Agency 306
Rocking	X	X	X	X	X
Shear/bed joint sliding with bond plus friction	X	X	X	X	X
Bed joint sliding with friction only					X
Diagonal tension				X	X
Toe crushing				X	X

where t=thickness of the wall; and v_m=masonry shear strength given by

$$v_m = 0.56v_t + 0.75\frac{P_D}{A} \tag{3}$$

where v_t=mortar shear strength determined by in-place shear tests (also known as ''push-tests''); P_D=dead load at the top of the pier; and A=mortared area, or equivalently, the pier's width (D) times its thickness (t). Note that the push-test measures the force required to displace a single brick by sliding on its bed joints.

Eqs. (2) and (3) are found in FEMA 178 and the CGSEEB. If Eq. (3) is substituted into Eq. (2), it gives

$$V_a = 0.373v_tA + 0.5P \tag{4}$$

A similar equation is found in FEMA 273 and FEMA 306, which acknowledges two forms of bed joints sliding: a stair-stepped diagonal crack as mentioned above, and sliding on a horizontal plane. In FEMA 273 and FEMA 306, both sliding behaviors are termed bed joint sliding with bond plus friction (V_{bjs1}), and the corresponding resistance is given by

$$V_{bjs1} = v_{me}A_n \tag{5}$$

where A_n=area of net mortared section; and v_{me}=bond plus friction strength of mortar, given by

$$v_{me} = \frac{0.75\left(0.75v_{te} + \frac{P_{CE}}{A_n}\right)}{1.5} \tag{6}$$

where v_{te}=mortar bond strength obtained from push tests.

Substituting Eq. (6) into Eq. (5), gives

$$V_{bjs1} = 0.375v_{te}A + 0.5P \tag{7}$$

which is identical to Eq. (4).

A special case of Eq. (6) is given in FEMA 306. At lateral drifts of 0.3 to 0.4%, a strength degradation most likely due to a complete erosion of the bond capacity has been observed experimentally. Thus, after the bond capacity in Eq. (6) has eroded, the strength is then based only on the friction portion of the equation. This behavior is termed ''bed joint sliding with friction only'' (V_{bjs2}), and is given by

$$V_{bjs2} = \frac{0.75\left(\frac{P_{CE}}{A_n}\right)}{1.5}(A_n) = 0.5P_{CE} \tag{8}$$

Note that Eq. (8) is not found in FEMA 178, FEMA 273, UCBC 1997, and the CGSEEB.

Diagonal Tension and Toe Crushing

Additionally, two other behavior modes, diagonal tension, and toe crushing, are recognized only in FEMA 273 and FEMA 306.

Typically, diagonal tension X-shaped cracking develops under high-compressive stress when strong mortar and weak masonry units are used. In this type of damage, double diagonal cracks form suddenly through the units, and the pier rapidly loses its vertical load carrying capacity. The force required to cause diagonal tension (V_{dt}) is given by

$$V_{dt} = f'_{dt}A_n(\beta)\left(1 + \frac{f_{ae}}{f'_{dt}}\right)^{1/2} \tag{9}$$

where f'_{dt}=diagonal tension strength, assumed as v_{me} in lieu of better available data; f_{ae}=expected vertical axial compressive stress; and $\beta = 0.67$ for $L/h_{\text{eff}} < 0.67$, $\beta = L/h_{\text{eff}}$ when $0.67 \leq L/h_{\text{eff}} \leq 1.0$, and $\beta = 1.0$ when $L/h_{\text{eff}} > 1$.

Under high-axial loads and the overturning moment due to a lateral load, a localized compression failure can occur at the toe of the pier. The force required to cause toe crushing (V_{tc}) is given by

$$V_{tc} = \alpha P_{CE}\left(\frac{L}{h_{\text{eff}}}\right)\left(1 - \frac{f_{ae}}{0.7f'_{me}}\right) \tag{10}$$

where f'_{me}=expected masonry compressive strength.

Table 2. Calculation of Pier In-Plane Seismic Resistance Based on Canadian Guidelines for the Seismic Evaluation of Existing Buildings

Pier	D/H	V_r (kN)	V_a (kN)	V_{cr} (kN)
Door	0.47	6.08	39.3	7.08
Central	1.48	34.5	64.5	36.6
Window	0.61	6.11	26.7	6.26

Theoretical Response Using Canadian Guidelines for Seismic Evaluation of Existing Buildings

Prior to the pseudo-dynamic tests, the expected strength of the URM specimen was assessed using the Canadian Guidelines for the Seismic Evaluation of Existing Buildings (CGSEEB) (NRC 1992) and masonry properties obtained from material tests. The CGSEEB procedure is very similar to the UCBC one.

First, the in-plane seismic resistance of each pier was determined, namely, the resistance to rocking, V_r, and shear failure, V_a

$$V_r = 0.9\frac{D}{H}P_D \tag{11}$$

and

$$V_a = v_mDt/1.5 \tag{12}$$

The lateral load required to initiate cracking the pier V_{cr} was calculated as

$$V_{cr} = f_t\frac{tD^2}{3H} + \frac{P_DD}{3H} \tag{13}$$

where f_t=tensile strength of the masonry.

The results of these calculations are summarized in Table 2. For all piers, the rocking resistance is less than the shear resistance, and the total rocking resistance for each shear wall is therefore the sum of the resistance of the individual components, i.e., $\Sigma V_r = 46.7$ kN.

Second, the maximum force transmitted by the diaphragm to the shear walls was determined. For this purpose, the total load tributary to the diaphragm, including walls perpendicular to the direction of motion W_d and the tributary load of each shear wall W_{wx} were calculated to be 114.5 and 21.1 kN, respectively. The corresponding expected in-plane seismic load F_{wx} on a shear wall for an effective velocity ratio, v' taken as 0.4 for the most severe seismic zone encountered in Canada, is

$$F_{wx} = v'(W_{wx} + W_d/2) = 31.3 \text{ kN} \tag{14}$$

Because this is less than the shear wall rocking resistance of 46.7 kN previously calculated, this specimen would theoretically be able to resist the highest-seismic lateral force expected in Canada.

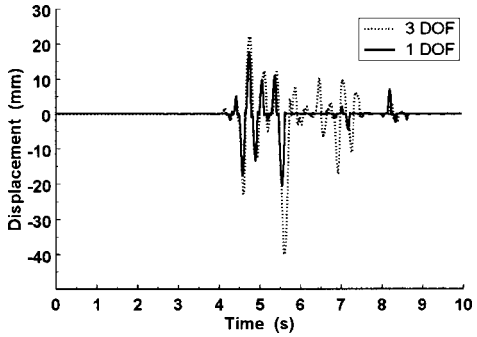

Fig. 6. End-wall rocking response obtained considering 3 DOF or 1 DOF models for the Northridge earthquake Newhall fire station record (peak ground acceleration of 0.583 g)

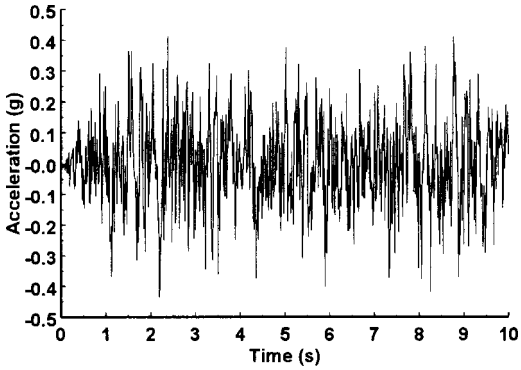

Fig. 7. Acceleration time history for La Malbaie (peak ground acceleration of 0.453 g)

However, this equation assumes that the ground motion applied at the diaphragm's edge is unamplified by the end walls.

Note that the force distributed to a shear wall cannot exceed

$$F_{wx} = v' W_{wx} + v_u D \tag{15}$$

where v = unit shear strength of the diaphragm; and D = diaphragm's width. In this case, the unit shear strength of a diagonal sheathing with straight overlay diaphragm is 29.8 kN/m based on values from the CGSEEB procedure. Thus, for a 3.66 m × 5.28 m diaphragm, the seismic lateral force distributed to the shear wall is limited by the shear yielding strength of the diaphragm

$$F_{wx} = 0.4(21.3) + 29.8(3.66) = 117.5 \text{ kN} \tag{16}$$

Experimental Procedure and Instrumentation

Pseudo-Dynamic Test Setup

A first logical actuator configuration for the test of interest here would be to use one actuator to excite the tributary mass at each end-wall location, and another to displace the tributary mass at the diaphragm center-span. This is referred to as a three degrees-of-freedom model (3 DOF). However, in light of the analytical results that show how wall response is largely driven by the diaphragm response, sufficiently accurate seismic response can be captured by using only a single actuator acting at the diaphragm center span, i.e., using a single-degree-of-freedom model (1 DOF). Analyses conducted to validate this concept and determine the effective tributary mass that would match the fundamental period of the specimen are presented elsewhere (Paquette and Bruneau 2002). However, results for the Northridge earthquake Newhall fire station record (a near-fault record with large peak-ground-velocity) are presented in Fig. 6. As shown in that figure, most of the instances and magnitudes of pier rocking observed using the 3 DOF analytical model are captured using the 1 DOF model. Given the supporting evidence from analytical studies, and the fact that using a single actuator results in a simpler test setup, with considerable savings, the 1 DOF configuration is used in this testing program.

Ground Motion

Nonlinear inelastic analyses were conducted to determine an appropriate seismic input motion representative of Eastern North America seismicity and that would initiate significant pier rocking from the diaphragm response. The selected input motion is a synthetic ground motion for La Malbaie, Canada, with a peak ground acceleration (PGA) of 0.453 g, as shown in Fig. 7. The simulated analytical shear wall response to La Malbaie × 2.0 produced the numerous desired pier-rocking cycles.

Test Setup and Instrumentation

The unreinforced brick masonry specimen was secured to a strong floor by four high-strength bolts affixed at each corner of the reinforced concrete foundation. A MTS hydraulic actuator was connected to the specimen's south wall at center span, and at the wood diaphragm level. The actuator was supported by a rigid steel reaction frame as shown in Fig. 8. The head of the actuator was connected on a built-up steel section made of plates welded together, and attached with four long steel rods running through the entire width of the building above and below the wood diaphragm and connected to a similar built-up steel section on the north wall. Those rods were used to avoid pulling on the south wall, and to instead push on the north wall when reverse loading was applied.

The testing plan was to subject the specimen to the same La Malbaie synthetic time history described previously, scaled to progressively increasing intensity. The pseudo-dynamic method was used for many of the tests conducted on the specimen. The characteristics of this on-line computer-controlled testing technique have been extensively described elsewhere (Shing and Mahin 1987a,b, 1990; Shing and Vannan 1990). In summary, this approach allows for the testing of structures or components under real earthquake excitations but at a relatively slow speed, thus allowing one to observe the evolution of damage. The dynamic characteristics of the structure (equivalent mass and damping) are

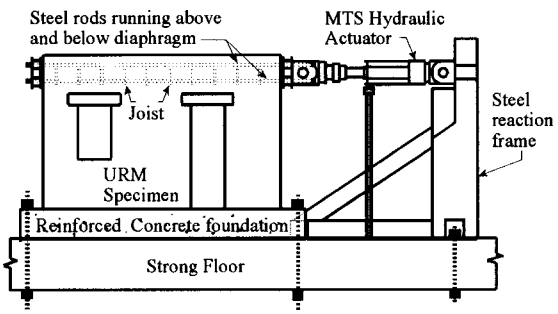

Fig. 8. Test setup

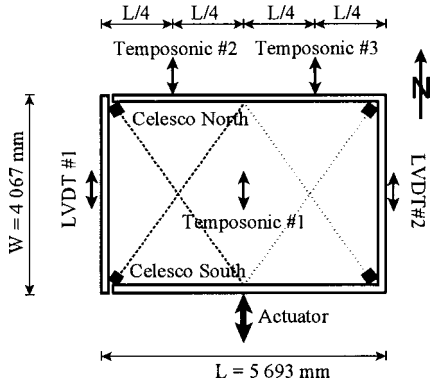

Fig. 9. Top view and location of temposonics, LVDTs, and Celescos

numerically simulated on a computer model, while the restoring force characteristics are directly measured from the tested specimens. Here, the pseudo-dynamic testing algorithm by Shing et al. (1991) was used.

The time-history response of the specimen was measured by a variety of instruments. As shown in Fig. 9, the displacement of the diaphragm was measured at the quarter points by temposonics, the midspan displacement being the controlling variable for the pseudo-dynamic test. The displacement of both shear walls at the diaphragm level was recorded by linear voltage displacement transducer (LVDT). Due to the limited number of instruments available, only the west shear wall of the specimen was closely instrumented during the early test runs. However, some tests were repeated with instruments moved to the east shear wall. As shown in Fig. 10, a pair of LVDT was placed on the central pier to monitor shear deformation. Also, the in-plane deformation of the diaphragm was measured by displacement transducers (Celesco) located diagonally across half of the diaphragm. Finally, as shown in Fig. 10, 12 special clip gauges were installed at expected crack locations around all the piers to record crack opening and closing during the pier's rocking cycle. All data were recorded automatically by a data acquisition system.

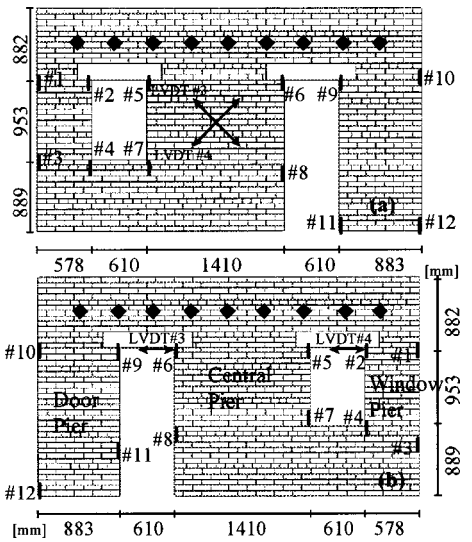

Fig. 10. Location of LVDTs and clip gauges: (a) west wall elevation and (b) east wall elevation

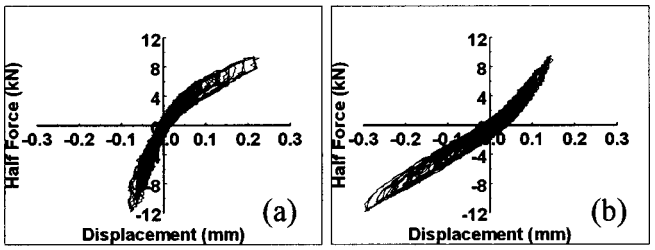

Fig. 11. Hysteretic response during La Malbaie×0.5 of (a) west wall and (b) east wall

Experimental Results

Description and visual observations made during testing are presented in this section. First, the specimen was subjected to a series of pseudo-dynamic simulated free vibration tests (MTS 1995) to determine the period of vibration of the specimen and its damping ratio. An initial displacement of 1 mm gave insufficient data points. Displacements of 2 and 3 mm yielded sufficient information to calculate the period and damping ratio that were found to be 0.12 s and 15%, respectively.

The specimen was then subjected to the first 10 s of La Malbaie earthquake multiplied by 0.25. During this test run, both shear walls and the diaphragm responded elastically. Then, the specimen was tested with La Malbaie×0.5. As shown in Fig. 11, a different stiffness response was noticeable for the two shear walls. Interestingly, the stiffness softening of each shear wall is also different depending on the direction of the force. The full-scale La Malbaie earthquake was then applied creating additional cracking. Clip gauges recorded maximum crack opening ranging from 0.18 to 4.00 mm. The earthquake excitation was then increased to La Malbaie×1.5; some cracking noise was heard and additional cracks were discovered. Sliding of the central pier was noticed on the west shear wall. All clip gauges, except two that were not located over a crack, recorded a maximum crack opening ranging from 0.5 to 8.0 mm, and rocking of the door pier was clearly evident. Finally, the specimen was subjected to La Malbaie×2. The hysteretic response of the west and east wall is shown in Figs. 12(a and b), respectively. Additional cracks on the shear walls and a longitudinal crack appeared between the 7th and 8th row of bricks on the north head wall. On the west wall, a triangular piece of wall surrounded by cracking started to separate due to the combined rocking and sliding motion of the central pier. Recorded maximum crack openings ranged from 2.5 to 13.0 mm. The pier's rocking motion is clearly shown in Fig. 13, where the crack opens when the force acts in one direction and remains closed in the reverse direction. The resulting crack pattern for the west and east wall is shown in Figs. 14(a and b), respectively.

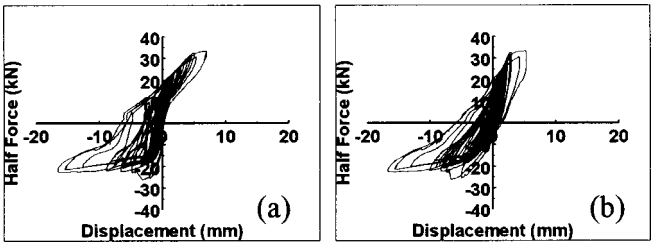

Fig. 12. Hysteretic response during La Malbaie×2.0 of (a) west wall and (b) east wall

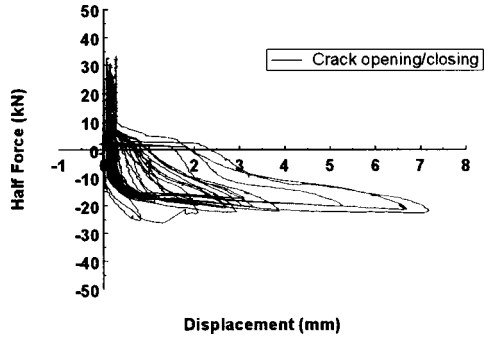

Fig. 13. Door pier rocking response during La Malbaie×2.0

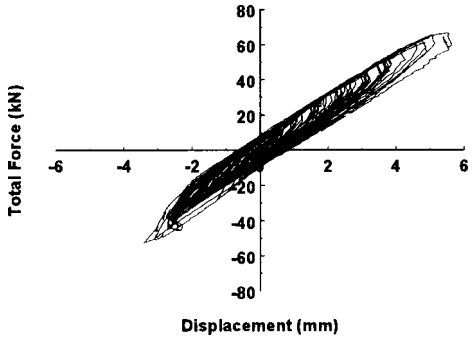

Fig. 15. Hysteretic response of wood diaphragm at center span during La Malbaie×2.0

The clip gauges monitoring the cracks on the west wall were then installed on the east wall, and the displacement transducers were moved on the eastern half of the diaphragm. The unreinforced masonry building was then retested with La Malbaie ×1.0 and ×1.5. The maximum crack opening varied from 0.5 to 1.3 mm, and from 0.5 to 2.9 mm for La Malbaie×1.0 and ×1.5, respectively.

As stated above, a different stiffness for the east and west walls was observed at the beginning, during low-intensity seismic motion. However, the hysteretic curves generated using La Malbaie×2.0 are very similar, as shown in Figs. 12(a and b). This suggests that the effect of continuous/discontinuous corners becomes somehow negligible during high-intensity seismic motion. It was also observed that the diaphragm remained elastic throughout the tests, as shown in Fig. 15.

Analysis of Results

Push Over Analyses

The single-story URM building specimen tested was designed in 1996, using the CGSEEB methodology to assess its strength and expected seismic response. Recall that the CGSEEB is essentially similar to the FEMA 178 Appendix C procedure, and Appendix 1 of the UCBC 1997. As the FEMA 273, and FEMA 306 documents became available after the specimen was constructed, it is worthwhile to compare the theoretical response of the URM specimen obtained from these various seismic evaluation procedures. Consequently, the strengths for each individual modes of behavior for each pier were calculated using the experimentally obtained compressive, tensile, and shear material properties reported in an earlier section, and summarized in Table 3.

Federal Emergency Management Agency 273

Following the procedure outlined in FEMA 273, rocking governs for all piers (the expected lateral strengths of each pier per each possible failure mode are listed in Table 3). For that mode of failure, piers are considered as deformation-controlled components, being able to sustain large lateral deflections as strengths remain almost constant. Thus, the lateral capacity for each shear wall is the summation of each individual pier rocking capacity, and is equal to 46.7 kN, a value identical to that computed using the CGSEEB, as reported in an earlier section.

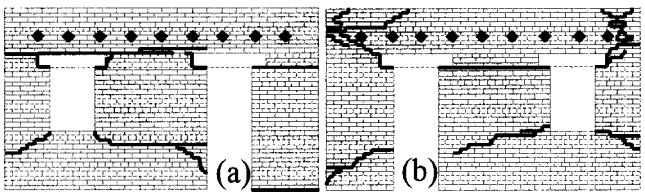

Fig. 14. Crack pattern after La Malbaie×2.0 (a) west wall and (b) east wall

Federal Emergency Management Agency 306

FEMA 306 gives a procedure to evaluate lateral capacity based on observed damage caused by an earthquake. As such, it requires us to use the effective height (h_{eff}) of pier reflecting the observed crack pattern. Therefore, the capacities for the individual modes of behavior for each pier shown in Table 3, were recalculated using the crack pattern observed after pseudo-dynamic tests. The effective height used and resulting capacities are presented in Table 4.

Based on the piers' aspect ratios and the applied vertical stresses, the governing modes of behavior are determined. According to FEMA 306, for piers with aspect ratio (L/h_{eff}) less or equal to 1.25, and for a vertical stress (f_{ae}) less than 0.69 MPa (100 psi), the predicted mode of failure is rocking if V_r or V_{tc} are the lowest values of V_r, V_{bjs1}, V_{bjs2}, V_{dt}, and V_{tc}. For the tested URM specimen, all piers have an aspect ratio less than 1.25 and V_r is the governing mode of failure, except for the central pier whose strength is governed by bed joint sliding with friction only, V_{bjs2}. In such a case, the lateral load capacity for each shear wall is given by the summation of the governing strength of each individual pier. For the west and east wall, this is 23.0 and 22.2 kN, respectively. Both rocking and bed joint sliding are considered to be deformation-controlled behaviors able to sustain large lateral deformations while strength remains almost constant.

Comparison with Experimental Results

The FEMA 273 nonlinear static procedure was used to establish the idealized nonlinear force-deflection relation for the wall, as

Table 3. Calculation of Pier Possible Behavior Mode Based on Federal Emergency Management Agency 273

Pier	Pier's height h (mm)	Rocking V_r (kN)	Bed joint sliding v_{bjs1} (kN)	Diagonal tension V_{dt} (kN)	Toe crushing V_{tc} (kN)
Door	1,842	6.08	39.8	24.5	6.70
Central	953	34.5	65.2	59.8	37.9
Window	953	6.11	27.0	16.6	6.72

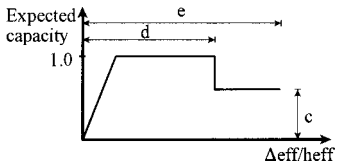

Fig. 16. FEMA 273 idealized normalized force-deflection relation

shown in Fig. 16. In this procedure, permissible deformations are established as drift percentages for primary elements (walls considered to be part of the lateral-force system) and secondary elements (walls not considered as part of the lateral-force-resisting system but supporting gravity loads) for the different performance levels of immediate occupancy (IO), life safety (LS), and collapse prevention (CP) as per Table 5. For comparison purposes, here, the walls are treated as primary elements. Permissible drift limits for the shear walls were calculated using an average pier's height and length. The expected capacities for FEMA 273 (46.7 kN) and FEMA 306 (23.0 and 22.2 kN for the west and east wall, respectively) are used. The idealized nonlinear force deflection is plotted against the hysteretic response of the west wall and east wall in Figs. 17(a and b), respectively.

Results and observations during the test show that all piers in the west wall started to rock during the first low-amplitudes tests. Then, upon reaching a maximum negative lateral load of approximately 29 kN during La Malbaie$\times$1.5 (negative meaning pushing towards the south wall), the central pier behavior gradually switched from rocking to bed joint sliding during La Malbaie $\times$2.0, reducing the strength to approximately 23 kN, which matches the push-over analysis results calculated with FEMA 306 in the preceding section, as shown in Fig. 17(a). However, when the force was acting in the opposite direction, the behavior was slightly different. During testing, the portion of the wall above the door pier was observed to lift, creating a gap across the entire width at the top of the door pier. Therefore, this pier became ineffective in providing resistance against lateral loads. That pier's share of gravity load resistance was thus transferred to the central pier, increasing its rocking resistance. The capacity of the west wall for a positive force is therefore given by adding the rocking capacity of the window pier (3.97 kN) to the increased rocking capacity of the central pier (approximately 35.1 kN), with no contribution from the door pier. A maximum strength of approximately 33 kN has been reached [Fig. 17(a)], and slightly higher values might have been obtained if testing had not stopped due to damage under negative lateral loads.

From test results and observations, the lateral capacity of the east wall for a positive force is given by the sum of the rocking capacity of each pier and equal to 34.95 kN. As shown in Fig. 17(b), a maximum lateral strength of approximately 33 kN was also reached for that wall. The lateral capacity for a negative force is slightly different. As observed during the test, both the door and window pier were rocking but the diaphragm was simply sliding on the central pier. Therefore, the estimated lateral strength is the rocking capacity of the door (5.48 kN) and window pier (3.77 kN) plus the strength of the diaphragm sliding on top of the central pier (10.5 kN), which adds up to 19.8 kN. As shown in Fig. 17(b), the maximum load reached is approximately 23 kN.

By looking at Fig. 17, a number of observations can be made. As noted in FEMA 307 (FEMA 1999b) (a document providing additional information on the basis and use of FEMA 306), the experimentally obtained displacements that occurred under a stable rocking mechanism exceed the proposed "*d*" drift value for the collapse of $0.4h_{\text{eff}}/L$, and equal to 0.52% for the primary element, as specified in FEMA 273. Furthermore, as also noted in FEMA 307 and observed here, the rocking capacity does not drop to a "*c*" value of 60% of the initial capacity as proposed by FEMA 273. Finally, FEMA 307 comments that a sequence of different behaviors is common in experiments. The rocking shifting to bed joint sliding for the central pier, observed when pushing the building in the south direction, is consistent with this expectation.

Given the reasonable agreement between experimental results and the above calculations which neglect the presence of a continuous corner at the east end, and comparing results for both building ends, it appears that pier continuity at the corner has no beneficial effect on behavior.

Table 4. Calculation of Pier Possible Behavior Mode Based on Federal Emergency Management Agency 306

Wall	Pier	h_{eff} (mm)	V_r (kN)	V_{bjs1} (kN)	V_{bjs2} (kN)	V_{dt} (kN)	V_{tc} (kN)
West	Door	1,842	6.08	39.8	7.05	24.5	6.73
	Central	1,335	24.6	65.2	12.95	59.8	27.3
	Window	1,469	3.97	27.0	5.6	16.6	4.34
East	Door	2,043	5.48	39.8	7.05	24.5	6.03
	Central	1,278	25.7	65.2	12.95	59.8	28.3
	Window	1,546	3.77	27.0	5.6	16.6	4.12

Conclusions

A full-scale one-story unreinforced brick masonry specimen having a flexible wood diaphragm was tested pseudo-dynamically. Tests results have shown that stable combined rocking and sliding mechanisms formed and large deformations developed without significant strength degradation. The diaphragm remained, however, essentially elastic throughout. The theoretical seismic response was calculated using different codified evaluation methodologies. It was found that the FEMA 273 procedure predicted the same behavior for the shear walls as the CGSEEB, i.e., a rocking mode for all piers but strengths in excess of experimentally obtained results. The FEMA 306 procedure gave results that closely matched the observed behavior. None of the codified procedure account for the presence of continuous corners, but this continuity was observed to have a negligible impact on the lateral strength of the shear wall during high intensity input motion.

Table 5. Federal Emergency Management Agency 273 Limiting Drift Values for Idealized Force-Deflection Relation

				Primary			Secondary	
Mode	*c* %	*d* %	*e* %	Immediate occupancy %	Life safety %	Collapse prevention %	Life safety %	Collapse prevention %
Bed-joint sliding	0.6	0.4	0.8	0.1	0.3	0.4	0.6	0.8
Rocking	0.6	$0.4h_{\text{eff}}/L$	$0.8h_{\text{eff}}/L$	0.1	$0.3h_{\text{eff}}/L$	$0.4h_{\text{eff}}/L$	$0.6h_{\text{eff}}/L$	$0.8h_{\text{eff}}/L$

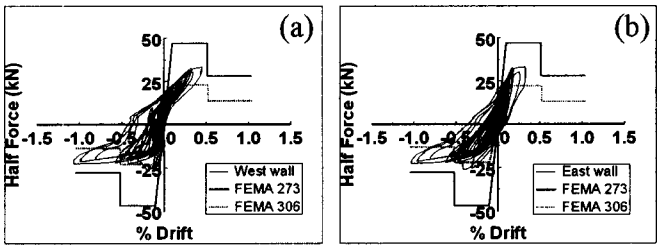

Fig. 17. Comparison with idealized force-deflection model using expected capacities from FEMA 273 and FEMA 306 during La Malbaie×2.0, for: (a) west wall and (b) east wall

Acknowledgments

The writers acknowledge the financial support provided by the Natural Science and Engineering Research Council of Canada (NSERC), Brampton Brick, Fitzgerald Building Supplies (1996) Limited, Ottawa Region Masonry Contractors Association, International Union of Brick Layers and Allied Craftsmen (Industrial Promotion Fund), Canadian Portland Cement Association, George and Asmussen Limited. However, conclusions and opinions expressed in this paper are those of the writers alone.

References

ABK, A joint venture. (1984). ''Methodology for mitigation of seismic hazards in existing unreinforced masonry buildings: The methodology.'' *Rep. ABK-TR-08*, Agbabian & Associates, S. B. Barnes & Associates, and Kariotis & Associates, El Segundo, Calif.

Bruneau, M. (1990). ''Preliminary report of structural damage from the Loma Prieta (San Francisco) earthquake of 1989 and pertinence to Canadian structural engineering practice.'' *Can. J. Civ. Eng.*, 17(2), 198–208.

Bruneau, M. (1994a). ''Seismic evaluation of unreinforced masonry buildings—A state-of-the-art report.'' *Can. J. Civ. Eng.*, 21(3), 512–539.

Bruneau, M. (1994b). ''State-of-the-art report on the seismic performance of unreinforced masonry buildings.'' *J. Struct. Eng.*, 120(1), 230–251.

Bruneau, M. (1995). ''Performance of masonry structures during the 1994, Northridge (L.A.) earthquake.'' *Can. J. Civ. Eng.*, 22(2), 378–402.

Costley, A. C., and Abrams, D. P. (1995). ''Dynamic response of unreinforced masonry buildings with flexible diaphragms.'' *Rep. No. UILU-ENG-95-2009*, Dept. of Civil Engineering, Univ. of Illinois at Urbana-Champaign, Urbana, Ill.

Canadian Standards Association (CSA). (1994). ''Masonry design for buildings.'' CSA Standard S304.1-94, *Canadian Standards Association*, Rexdale, Ont., Canada.

Federal Emergency Management Agency (FEMA) 178. (1992). ''NEHRP handbook for the seismic evaluation of existing buildings.'' *Building seismic safety council*, FEMA, Washington, D.C.

FEMA 273. (1997). ''NEHRP guidelines for the seismic rehabilitation of buildings.'' *Building seismic safety council*, FEMA, Washington, D.C.

FEMA 306. (1999a). ''Evaluation of earthquake damaged concrete and masonry wall buildings, basic procedures manual.'' *The partnership for response and recovery*, FEMA, Washington, D.C.

FEMA 307. (1999b). ''Evaluation of earthquake damaged concrete and masonry wall buildings, technical resources.'' *The patnership for response and recovery*, FEMA, Washington, D.C.

International Conference of Building Officials (ICBO). (1997). *Uniform code for building conservation*, International Conference of Building Officials, Whittier, Calif.

(MTS). (1995). *TestStar program for pseudodynamic testing. Pseudodynamic software user's manual*, MTS Systems Corporation, Eden Prairie, Minn.

National Research Council (NRC). (1992). *Guidelines for seismic evaluation of existing buildings*, Institute for Research in Construction, National Research Council, Ottawa.

Paquette, J., and Bruneau, M. (2002). ''Seismic testing of unreinforced masonry with flexible diaphragm.'' Ottawa Carleton Earthquake Engineering Research Centre, *Rep. No. OCEERC-02-25*, Ottawa.

Rutherford and Chekene (1991). ''Damage to unreinforced masonry buildings in the Loma Prieta earthquake of October 17, 1989.'' *California Seismic Safety Commission*, Sacramento, Calif., 38.

Shing, P. B., and Mahin, S. A. (1987a). ''Cumulative experimental errors in pseudo-dynamic tests.'' *Earthquake Eng. Struct. Dyn.*, 15, 409–424.

Shing, P. B., and Mahin, S. A. (1987b). ''Elimination of spurious higher-mode response in pseudo-dynamic tests.'' *Earthquake Eng. Struct. Dyn.*, 15, 425–445.

Shing, P. B., and Mahin, S. A. (1990). ''Experimental error effects in pseudo-dynamic tests.'' *J. Eng. Mech.*, 116(4), 805–821.

Shing, P. B., and Vannan, M. (1990). ''On the accuracy of implicit algorithm for pseudo-dynamic tests.'' *Earthquake Eng. Struct. Dyn.*, 19, 631–651.

Shing, P. B., Vannan, M., and Carter, E. (1991). ''Implicit time integration for pseudo-dynamic tests.'' *Earthquake Eng. Struct. Dyn.*, 20, 551–576.